*Stanford Exploration Project, Report 89, November 12, 1997, pages 111–134*

# Amplitude preserving offset continuation in theory
# Part 2: Solving the equation

*Sergey Fomel*[1]

***keywords:*** *DMO, continuation, amplitudes*


## ABSTRACT

I consider an initial value problem for the offset continuation (OC) equation introduced in Part One of this paper (SEP–84). The solutions of this problem create integral-type OC operators in the time-space domain. Moving to the frequency-wavenumber and log-stretch domain, I compare the obtained operators with the well-known Fourier DMO operators. This comparison links the theory of DMO with the advanced theory of offset continuation.


## INTRODUCTION

Offset continuation (OC) is a process that transforms common-offset seismic data from one constant offset to another. Introduced initially by Deregowski and Rocca (1981) and Bolondi et al. (1982), the OC concept stimulated the early stages of dip moveout (DMO). However, its direct implementation for interpolating and regularizing seismic data was not as successful as that of DMO by Fourier transform (Hale, 1984) and other versions of DMO (Hale, 1991b). One of the reasons was the approximate nature of Bolondi's OC algorithm, limiting the range of its application to small offsets and reflector dips. Biondi and Chemingui (1994) and Bagaini et al. (1994) recently derived an improved integral version of offset continuation, which provides a correct kinematics of offset continuation in the constant velocity media.

In Part One of this paper (Fomel, 1995), I introduced a revised partial differential equation that describes the offset continuation process in time-offset-midpoint space. Under a constant velocity assumption, the equation was proven to provide correct geometry and meaningful amplitudes of the continued reflection events.

This part of the paper starts with an initial value (Cauchy-type) problem for the OC equation. I solve this problem to obtain explicit integral-type operators of offset

[1]**email:** sergey@sep.stanford.edu

continuation in the time-space domain. In the rest of the paper, I consider DMO as a special case of offset continuation for the output offset equal to zero and compare the new OC operators with those of the canonical DMO: Hale's Fourier-domain DMO (Hale, 1984) and Liner's log-stretch DMO (Liner, 1990).

Here I do not focus specifically on the amplitude preservation properties of offset continuation, assuming that the asymptotic analysis of the OC amplitudes (Fomel, 1995) applies both to the OC equation and to its solutions.

## THE CAUCHY PROBLEM

Throughout this paper I refer to the equation (Fomel, 1994, 1995)

$$h \left( \frac{\partial^2 P}{\partial y^2} - \frac{\partial^2 P}{\partial h^2} \right) = t_n \, \frac{\partial^2 P}{\partial t_n \, \partial h} \; , \tag{1}$$

where $h$ is the half-offset, $y$ is the midpoint, and $t_n$ is the time coordinate after the NMO correction. Equation (1) describes a continuous process of reflected wavefield continuation in the time-offset-midpoint domain. In order to find an integral-type operator that performs the one-step offset continuation, I consider the following initial value (Cauchy) problem for equation (1):

*Given a post-NMO constant-offset section at half-offset $h_1$*

$$\left. P(t_n,h,y) \right|_{h=h_1} = P_1^{(0)}(t_n,y) \tag{2}$$

*and its first-order derivative with respect to offset*

$$\left. \frac{\partial P(t_n,h,y)}{\partial h} \right|_{h=h_1} = P_1^{(1)}(t_n,y) \; , \tag{3}$$

*find the corresponding gather $P^{(0)}(t_n,y)$ at offset $h$.*

Equation (1) belongs to the hyperbolic type, with the offset coordinate $h$ being a "time-like" variable, and the midpoint coordinate $y$ and the time $t_n$ being "space-like" variables. The last condition (3) is required for the initial value problem to be well-posed (Courant, 1962). From a physical point of view, its role is to separate the two different wave-like processes embedded in equation (1) and analogous to inward and outward wave propagation. We will associate the first process with continuation to a larger offset, and the second one with continuation to a smaller offset. Though the offset derivatives of data are not measured in practice, they can be estimated from the data at neighboring offsets by a finite-difference approximation. Eliminating condition (3) in the offset continuation problem is a challenging task that requires separate consideration.

## THE INTEGRAL OPERATOR FOR OFFSET CONTINUATION

The integral solution of problem (1)-(3) is obtained in Appendix A with the help of the classic methods of mathematical physics. It takes the explicit form

$$\begin{aligned} P(t_n,h,y) &= \iint P_1^{(0)}(t_1,y_1)\,G_0(t_1,h_1,y_1;t_n,h,y)\,dt_1\,dy_1 \\ &+ \iint P_1^{(1)}(t_1,y_1)\,G_1(t_1,h_1,y_1;t_n,h,y)\,dt_1\,dy_1\;, \end{aligned} \tag{4}$$

where the "Green's functions" $G_0$ and $G_1$ are expressed as

$$G_0(t_1,h_1,y_1;t_n,h,y) = \mathrm{sign}(h-h_1)\,\frac{H(t_n)}{\pi}\,\frac{\partial}{\partial t_n}\left\{\frac{H(\Theta)}{\sqrt{\Theta}}\right\}\;, \tag{5}$$

$$G_1(t_1,h_1,y_1;t_n,h,y) = \mathrm{sign}(h-h_1)\,\frac{H(t_n)}{\pi}\,h\,\frac{t_n}{t_1^2}\left\{\frac{H(\Theta)}{\sqrt{\Theta}}\right\}\;, \tag{6}$$

and the parameter $\Theta$ is

$$\Theta(t_1,h_1,y_1;t_n,h,y) = \left(h_1^2/t_1^2 - h^2/t_n^2\right)\,\left(t_1^2-t_n^2\right) - (y_1-y)^2\;. \tag{7}$$

$H$ stands for the Heavyside step-function.

From formulas (5) and (6) one can see that the impulse response of the offset continuation operator is discontinuous in the time-offset-midpoint space on a surface defined by the equality

$$\Theta(t_1,h_1,y_1;t_n,h,y) = 0 \tag{8}$$

that describes the "wavefronts" of the offset continuation process. In terms of the theory of characteristics (Courant, 1962), the surface $\Theta = 0$ corresponds to the characteristic conoid formed by bi-characteristics of equation (1) – "time rays" (Fomel, 1995) emerging from the point $\{t_n,h,y\} = \{t_1,h_1,y_1\}$ (Figure 1).

As a second-order differential equation of the hyperbolic type, equation (1) describes two different processes. The first process is "forward" continuation from smaller to larger offsets; the second one is "reverse" continuation in the opposite direction. These two processes are clearly separated in the high-frequency asymptotics of operator (4). To obtain the asymptotic representation, it is sufficient to note that $\frac{1}{\sqrt{\pi}}\,\frac{H(t)}{\sqrt{t}}$ is the impulse response of the causal half-order integration operator, and that $\frac{H(t^2-a^2)}{\sqrt{t^2-a^2}}$ is asymptotically equivalent to $\frac{H(t-a)}{\sqrt{2a}\,\sqrt{t-a}}$ $(t,a>0)$. Thus, the asymptotic form of the integral offset continuation operator becomes

$$\begin{aligned} P^{(\pm)}(t_n,h,y) &= \mathbf{D}_{\pm t_n}^{1/2} \int w_0^{(\pm)}(\xi;h_1,h,t_n)\,P_1^{(0)}(\theta^{(\pm)}(\xi;h_1,h,t_n),y_1-\xi)\,d\xi\;\pm \\ &\pm\; \mathbf{I}_{\pm t_n}^{1/2} \int w_1^{(\pm)}(\xi;h_1,h,t_n)\,P_1^{(1)}(\theta^{(\pm)}(\xi;h_1,h,t_n),y_1-\xi)\,d\xi\;. \end{aligned} \tag{9}$$

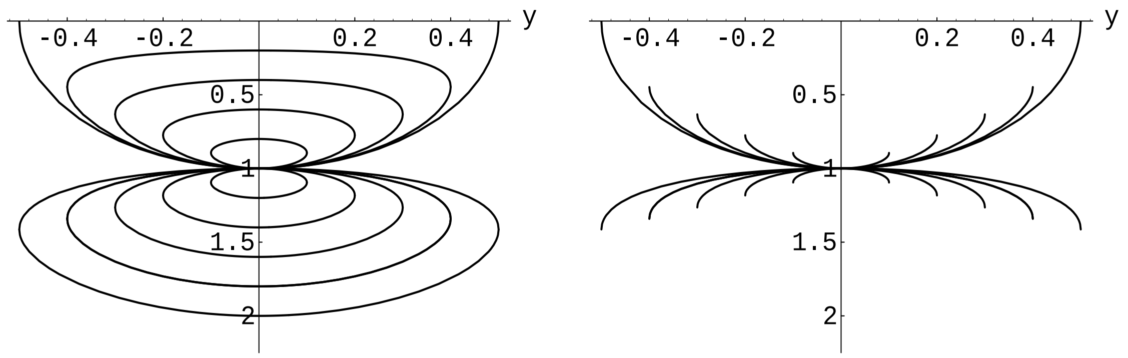


Figure 1: Constant-offset sections of the characteristic conoid - "offset continuation fronts" (left), and branches of the conoid used in the integral OC operator (right). The upper part of the plots (small times) corresponds to continuation to smaller offsets; the lower part (large times) corresponds to larger offsets. sergey1-offcon [CR]

Here the signs "+" and "−" correspond to the type of continuation (the sign of $h - h_1$); $\mathbf{D}^{1/2}_{\pm t_n}$ and $\mathbf{I}^{1/2}_{\pm t_n}$ stand for the operators of causal and anticausal half-order differentiation and integration applied with respect to the time variable $t_n$; the summation paths $\theta^{(\pm)}(\xi; h_1, h, t_n)$ correspond to the two non-negative sections of the characteristic conoid (8) (Figure 1):

$$t_1 = \theta^{(\pm)}(\xi; h_1, h, t_n) = \frac{t_n}{h} \sqrt{\frac{U \pm V}{2}}\;, \tag{10}$$

where $U = h^2 + h_1^2 - \xi^2$, and $V = \sqrt{U^2 - 4\,h^2\,h_1^2}$; $\xi$ is the midpoint separation (the integration parameter); and $w_0^{(\pm)}$ and $w_1^{(\pm)}$ are the following weighting functions:

$$w_0^{(\pm)} = \frac{1}{\sqrt{2\,\pi}} \frac{\theta^{(\pm)}(\xi; h_1, h, t_n)}{\sqrt{t_n\,V}}\;, \tag{11}$$

$$w_1^{(\pm)} = \frac{1}{\sqrt{2\,\pi}} \frac{\sqrt{t_n}\,h_1}{\sqrt{V}\,\theta^{(\pm)}(\xi; h_1, h, t_n)}\;. \tag{12}$$

Expression (10) for the summation path of the OC operator was obtained previously by Stovas and Fomel (1993) and Biondi and Chemingui (**?**). A somewhat different form of it is proposed by Bagaini et al. (1994). I describe the kinematic interpretation of formula (10) in Appendix B.

The limit of expression (10) for the output offset $h$ approaching zero can be evaluated by L'Hospitale's rule. As one would expect, it coincides with the well-known expression for the summation path of the integral DMO operator (Deregowski and Rocca, 1981)

$$t_1 = \theta^{(-)}(\xi; h_1, 0, t_n) = \lim_{h \to 0} \frac{t_n}{h} \sqrt{\frac{U - V}{2}} = \frac{t_n\, h_1}{\sqrt{h_1^2 - \xi^2}} \; . \tag{13}$$

## OFFSET CONTINUATION AND DMO

Dip moveout represents a particular case of offset continuation for the output offset equal to zero. In this section, I consider the DMO case separately in order to compare the solutions of equation (1) with the Fourier-domain DMO operators, which have been the standard for DMO processing since Hale's outstanding work (**?**).

Starting from equations (A-14)-(A-16) in Appendix A and setting the output offset to zero, we obtain the following DMO-like integral operators in the $t$–$k$ domain:

$$\widetilde{P}(t_0, 0, k) = H(t_0)\, \left(\widetilde{P}_0(t_0, k) + t_0\, \widetilde{P}_1(t_0, k)\right) \; , \tag{14}$$

where

$$\widetilde{P}_0(t_0, k) = -\frac{\partial}{\partial t_0} \int_{t_0}^{\infty} \widetilde{P}_1^{(0)}\left(|t_1|\,, k\right)\; J_0\left(\frac{k\, h_1}{t_1}\, \sqrt{t_1^2 - t_0^2}\right)\, dt_1 \; , \tag{15}$$

$$\widetilde{P}_1(t_0, k) = -\int_{t_0}^{\infty} h_1\, \widetilde{P}_1^{(1)}\left(|t_1|\,, k\right)\; J_0\left(\frac{k\, h_1}{t_1}\, \sqrt{t_1^2 - t_0^2}\right)\, \frac{dt_1}{t_1^2} \; , \tag{16}$$

thje wavenumber $k$ corresponds to the midpoint axis $y$, and $J_0$ is the zero-order Bessel function. The Fourier transform of (15) and (16) with respect to the time variable $t_0$ reduces to known integrals (Gradshtein and Ryzhik, 1994) and creates explicit DMO-type operators in the frequency-wavenumber domain, as follows:

$$\widetilde{\widetilde{P}}_0(\omega_0, k) = i \int_{-\infty}^{\infty} \widetilde{P}_1^{(0)}\left(|t_1|\,, k\right)\; \frac{\sin\left(\omega_0\, |t_1|\, A\right)}{A}\, dt_1 \; , \tag{17}$$

$$\widetilde{\widetilde{P}}_1(\omega_0, k) = i \int_{-\infty}^{\infty} h_1\, \widetilde{P}_1^{(1)}\left(|t_1|\,, k\right)\; \frac{\sin\left(\omega_0\, |t_1|\, A\right)}{A} \frac{dt_1}{t_1^2} \; , \tag{18}$$

where

$$A = \sqrt{1 + \frac{(k\, h_1)^2}{(\omega_0\, t_1)^2}} \; , \tag{19}$$

$$\widetilde{\widetilde{P}}_j(\omega_0, k) = \int \widetilde{P}_j(t_0, k)\, \exp(i\omega_0 t_0)\, dt_0 \; . \tag{20}$$

It is curious to note that the first term of the continuation to zero offset (17) coincides exactly with the imaginary part of Hale's DMO operator (Hale, 1984). However, unlike Hale's, operator (14) is causal, which means that its impulse response does not continue to negative times. The non-causality of Hale's DMO and related issues are discussed in more detail by Stovas and Fomel (1993). I include a brief summary of this discussion in Appendix C.

Though Hale's DMO is known to provide correct reconstruction of the geometry of zero-offset reflections, it doesn't account properly for the amplitude changes (Black et al., 1993). The preceding section of this paper shows that the additional contribution to the amplitude is contained in the second term of the OC operator (4), which transforms to the second term in the DMO operator (14). Note that this term vanishes at the input offset equal to zero, which represents the case of the inverse DMO operator.

Considering the inverse DMO operator as the continuation from zero offset to a non-zero offset, we can obtain its representation in the $t-k$ domain from equations (A-14)-(A-16) as

$$\widetilde{P}(t_n,h,k) = H(t_n)\frac{\partial}{\partial t_n}\int_0^{t_n} \widetilde{P}_0\left(|t_0|\,,k\right)\, J_0\left(\frac{k\,h}{t_n}\sqrt{t_n^2-t_0^2}\right)\,dt_0\;, \tag{21}$$

Fourier transforming (21) with respect to the time variable $t_0$ (20), we get the Fourier-domain version of the "amplitude-preserving" inverse DMO:

$$\widetilde{P}(t_n,h,k) = \frac{H(t_n)}{2\,\pi}\,\frac{\partial}{\partial t_n}\int_{-\infty}^{\infty} \widetilde{\widetilde{P}}_0(\omega_0,k)\,\frac{\sin\left(\omega_0\,|t_n|\,A\right)}{\omega_0\,A}\,d\omega_0\;, \tag{22}$$

$$A = \sqrt{1+\frac{(k\,h)^2}{(\omega_0\,t_n)^2}}\;. \tag{23}$$

Comparing operator (22) with Ronen's version of inverse DMO (Ronen, 1987), one can see that if Hale's DMO is denoted by $\mathbf{D}_{t_0}\,\mathbf{H}$, then Ronen's inverse DMO is $\mathbf{H^T}\,\mathbf{D}_{-t_0}$, while the amplitude-preserving inverse (22) is $\mathbf{D}_{t_n}\,\mathbf{H^T}$. Here $\mathbf{D}_t$ is the derivative operator $\left(\frac{\partial}{\partial t}\right)$, and $\mathbf{H^T}$ stands for the adjoint operator, defined by the dot-product test

$$(\mathbf{Hm},\mathbf{d}) = (\mathbf{m},\mathbf{H^T d}), \tag{24}$$

where the parentheses denote the dot product (in the $L_2$ sense):

$$(\mathbf{m_1},\mathbf{m_2}) = \int\!\!\int m_1(t_n,y)\,m_2(t_n,y)\,dt_n\,dy\;. \tag{25}$$

In high-frequency asymptotics, the amplitude difference between the two inverses is simply the Jacobian term $\frac{d\,t_0}{d\,t_n}$, asymptotically equal to $\frac{t_0}{t_n}$. This difference corresponds exactly to the difference between Black's definition of amplitude preservation (Black et al., 1993) and the definition used in Born DMO (Liner, 1991; Bleistein, 1990), as discussed in (Fomel, 1995). While operator (22) preserves amplitudes in the Born DMO sense, Ronen's inverse satisfies Black's amplitude preservation criteria. This means Ronen's operator implies that the "geometric spreading" correction (multiplication by time) has been performed on the data prior to DMO.

To construct a one-term DMO operator, thus avoiding the estimation of the offset derivative in (12), let us consider the problem of inverting the inverse DMO operator (22). One of the possible approaches to this problem is the least-square iterative inversion, as proposed by Ronen (1987). This requires constructing the adjoint operator, which is Hale's DMO (or its analogue) in the case of Ronen's method. The iterative least-square approach can account for irregularities in the data geometry (Ronen et al., 1991; Ronen, 1994) and boundary effects, but it is computationally expensive because of the multiple application of the operators. An alternative approach is the asymptotic inversion, which can be viewed as a special case of preconditioning the adjoint operator (Liner and Cohen, 1988; Chemingui and Biondi, 1995). The goal of the asymptotic inverse is to reconstruct the geometry and the amplitudes of the reflection events in the high-frequency asymptotic limit.

According to Beylkin's theory of asymptotic inversion, also known as the *generalized Radon transform* (Beylkin, 1985), two operators of the form

$$D(\omega) = \int X(t,\omega)\, M(t)\, \exp\left[i\omega\phi(t,\omega)\right]\, dt \tag{26}$$

and

$$\widetilde{M}(t) = \int Y(t,\omega)\, D(\omega)\, \exp\left[-i\omega\phi(t,\omega)\right]\, d\omega \tag{27}$$

make a pair of asymptotically inverse operators if

$$X(t,\omega)\, Y(t,\omega) = \frac{Z(t,\omega)}{2\,\pi}\;, \tag{28}$$

where $Z$ is the "Beylkin determinant"

$$Z(t,\omega) = \left|\frac{\partial\omega}{\partial\hat{\omega}}\right| \text{ for } \hat{\omega} = \omega\,\frac{\partial\phi(t,\omega)}{\partial t}\;. \tag{29}$$

With respect to the high-frequency asymptotic representation, we can recast (22) to the equivalent form by moving the time derivative under the integral sign:

$$\widetilde{P}(t_n,k) \approx \frac{H(t_n)}{2\,\pi}\,\mathrm{Re}\left[\int_{-\infty}^{\infty} A^{-2}\,\widetilde{\widetilde{P}}_0(\omega_0,k)\,\exp\left(-i\omega_0\,|t_n|\,A\right)\, d\omega_0\right] \tag{30}$$

Now the asymptotic inverse of (30) is evaluated by means of Beylkin's method (26)-(27), which leads to an amplitude-preserving one-term DMO operator of the form

$$\widetilde{\widetilde{P}}_0(\omega_0,k) = \mathrm{Im}\left[\int_{-\infty}^{\infty} B\widetilde{P}_1^{(0)}\left(|t_1|\,,k\right)\,\exp\left(i\omega_0\,|t_1|\,A\right)\, dt_1\right]\;, \tag{31}$$

where

$$B = A^2 \frac{\partial}{\partial \omega_0} \left( \omega_0 \, \frac{\partial (t_n \, A)}{\partial t_n} \right) = A^{-1} \, (2 \, A^2 - 1) \; . \tag{32}$$

The amplitude factor (32) corresponds exactly to that of Born DMO (Bleistein, 1990) in full accordance with the conclusions of Fomel's asymptotic analysis of the offset continuation amplitudes (1995). An analogous result can be obtained with the different definition of amplitude preservation proposed by Black et al. (1993). In the time-and-space domain, the operator asymptotically analogous to (31) is found by applying either the stationary phase technique (Liner, 1990; Black et al., 1993) or Goldin's method of discontinuities (Goldin, 1988, 1990), which is the time-and-space analogue of Beylkin's asymptotic inverse theory (Stovas and Fomel, 1993). The time-and-space asymptotic DMO operator takes the form

$$P_0(t_0, y) = \mathbf{D}_{-t_0}^{1/2} \int w_0(\xi; h_1, t_0) \, P_1^{(0)}(\theta^{(-)}(\xi; h_1, 0, t_0), y_1 - \xi) \, d\xi \; , \tag{33}$$

where the weighting function $w_0$ is defined as

$$w_0(\xi; h_1, t_0) = \sqrt{\frac{t_0}{2\,\pi}} \, \frac{h_1 \, (h_1^2 + \xi^2)}{(h_1^2 - \xi^2)^2} \; . \tag{34}$$

## OFFSET CONTINUATION AND DMO IN THE LOG-STRETCH DOMAIN

The log-stretch transform, proposed by Bolondi et al. (1982) and further developed by many other researchers, has proven a useful tool in DMO and OC processing. Applying the log-stretch transform of the form

$$\sigma = \ln \left| \frac{t_n}{t_*} \right| \; , \tag{35}$$

where $t_*$ is an arbitrarily chosen time constant, eliminates the time dependence of the coefficients in equation (1) and therefore makes this equation invariant to time shifts. After the double Fourier transform with respect to the midpoint coordinate $y$ and to the transformed (log-stretched) time coordinate $\sigma$, the partial differential equation (1) takes the form of an ordinary differential equation,

$$h \left( \frac{d^2 \widehat{\widehat{P}}}{dh^2} + k^2 \, \widehat{\widehat{P}} \right) = i\Omega \, \frac{d\widehat{\widehat{P}}}{dh} \; , \tag{36}$$

where

$$\widehat{\widehat{P}}(h) = \int\int P(t_n = t_* \exp(\sigma), h, y) \exp(i\Omega\sigma - iky)\, d\sigma\, dy\ . \tag{37}$$

Equation (36) has the known general solution, expressed in terms of cylinder functions of complex order $\lambda = \frac{1+i\Omega}{2}$ (Watson, 1952):

$$\widehat{\widehat{P}}(h) = C_1(\lambda)\,(kh)^\lambda\, J_{-\lambda}(kh) + C_2(\lambda)\,(kh)^\lambda\, J_\lambda(kh)\ , \tag{38}$$

where $J_{-\lambda}$ and $J_\lambda$ are Bessel functions, and $C_1$ and $C_2$ stand for some arbitrary functions of $\lambda$ that don't depend on $k$ and $h$.

In the general case of offset continuation, $C_1$ and $C_2$ are constrained by the two initial conditions (2) and (3). In the special case of continuation from zero offset, we can neglect the second term in (38) as vanishing at the zero offset. The remaining term defines the following operator of inverse DMO in the $\Omega, k$ domain:

$$\widehat{\widehat{P}}(h) = \widehat{\widehat{P}}(0)\, Z_\lambda(kh)\ , \tag{39}$$

where $Z_\lambda$ is the analytic function

$$Z_\lambda(x) = \Gamma(1-\lambda)\, \left(\frac{x}{2}\right)^\lambda\, J_{-\lambda}(x) = \sum_{n=0}^{\infty} \frac{(-1)^n}{n!}\, \frac{\Gamma(1-\lambda)}{\Gamma(n+1-\lambda)}\, \left(\frac{x}{2}\right)^{2n}\ . \tag{40}$$

The DMO operator now can be derived as the inversion of operator (39), which is a simple multiplication by $1/Z_\lambda(kh)$. Therefore, offset continuation becomes a multiplication by $Z_\lambda(kh_2)/Z_\lambda(kh_1)$ (the cascade of two operators). This fact demonstrates an important advantage of moving to the log-stretch domain: both offset continuation and DMO are simple filter multiplications in the Fourier domain of the log-stretched time coordinate.

In order to compare operator (39) with the known versions of log-stretch DMO, it is necessary to derive its asymptotic representation for high frequencies $\Omega$. The required asymptotics follows directly from the definition of function $Z_\lambda$ in (40) and the known asymptotic representation for a Bessel function of high order (Watson, 1952):

$$J_\lambda(\lambda z) \overset{\lambda\to\infty}{\approx} \frac{(\lambda z)^\lambda\, \exp\left(\lambda\, \sqrt{1-z^2}\right)}{e^\lambda\, \Gamma(\lambda+1)\, (1-z^2)^{1/4}\, \left\{1+\sqrt{1-z^2}\right\}^{\sqrt{1-z^2}}}\ . \tag{41}$$

Substituting approximation (41) into (40) and considering the high-frequency limit of the resultant expression yields

$$Z_\lambda(kh) \approx \left\{\frac{1+\sqrt{1-\left(\frac{kh}{\lambda}\right)^2}}{2}\right\}^\lambda \frac{\exp\left(\lambda\left[1-\sqrt{1-\left(\frac{kh}{\lambda}\right)^2}\right]\right)}{\left(1-\left(\frac{kh}{\lambda}\right)^2\right)^{1/4}} \approx F(\epsilon)\, e^{i\Omega\,\psi(\epsilon)}\;, \quad (42)$$

where $\epsilon$ denotes the ratio $\frac{2\,k\,h}{\Omega}$,

$$F(\epsilon) = \sqrt{\frac{1+\sqrt{1+\epsilon^2}}{2\sqrt{1+\epsilon^2}}}\;\exp\left(\frac{1-\sqrt{1+\epsilon^2}}{2}\right)\;, \quad (43)$$

and

$$\psi(\epsilon) = \frac{1}{2}\left(1-\sqrt{1+\epsilon^2}+\ln\left(\frac{1+\sqrt{1+\epsilon^2}}{2}\right)\right)\;. \quad (44)$$

Asymptotic representation (42) is valid for large frequency $\Omega$ and $|\epsilon| \leq 1$. It can be shown that the phase function $\psi$ defined in (44) coincides precisely with the analogous term in Liner's "exact log DMO" (Liner, 1990), which was proven to provide the correct geometric properties of DMO. However, the amplitude term $F(\epsilon)$ is different from that of Liner's DMO because of the difference in the amplitude preservation properties.

A number of approximate log DMO operators have been proposed in the literature. As shown by Liner, all of them but "exact log DMO" distort the geometry of reflection effects at large offsets. This fact is caused by the implied approximations of the true phase function $\psi$. Bolondi's OC operator (Bolondi et al., 1982) implies $\psi(\epsilon) \approx -\frac{\epsilon^2}{8}$; Notfors DMO (Notfors and Godfrey, 1987) implies $\psi(\epsilon) \approx 1-\sqrt{1+(\epsilon/2)^2}$; and "full DMO" (Bale and Jakubowicz, 1987) has $\psi(\epsilon) \approx \frac{1}{2}\ln\left[1-(\epsilon/2)^2\right]$. All these approximations are valid for small $\epsilon$ (small offsets or small reflector dips) and have errors of the order of $\epsilon^4$ (Figure 2). The range of validity of Bolondi's operator is discussed in more detail in (Fomel, 1995).

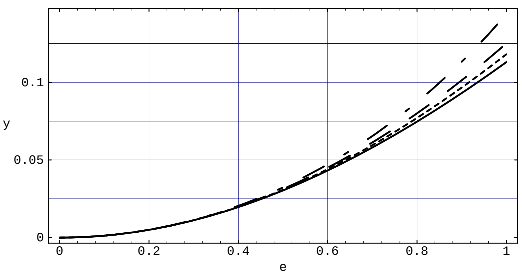


Figure 2: Phase functions of the log DMO operators. Solid line: exact log DMO; dashed line: Bolondi's OC; dashed-dotted line: Bale's full DMO; dotted line: Notfors DMO. $\boxed{\text{sergey1-offpha}}$ [CR]

In practice, seismic data are often irregularly sampled in space, but regularly sampled in time. This makes it attractive to apply offset continuation and DMO operators in the $\{\Omega, y\}$ domain, where the frequency $\Omega$ corresponds to the log-stretched time, and $y$ is the midpoint coordinate. Performing the inverse Fourier transform on the spatial frequency transforms the inverse DMO operator (39) to the $\{\Omega, y\}$ domain, where the filter multiplication becomes a convolutional operator:

$$\widehat{P}(\Omega,h,y) = \frac{\widehat{F}(\Omega)}{\sqrt{2\,\pi}} \int_{|\xi|<h} \frac{h}{h^2-\xi^2}\,\widehat{P_0}(\Omega,y-\xi)\,\exp\left(-\frac{i\Omega}{2}\,\ln\left(1-\frac{\xi^2}{h_1^2}\right)\right)\,d\xi\;. \qquad (45)$$

Here $\widehat{F}(\Omega)$ is a high-pass frequency filter:

$$\widehat{F}(\Omega) = \frac{\Gamma(1/2 - i\Omega/2)}{\sqrt{1/2}\,\Gamma(-i\Omega/2)}\;. \qquad (46)$$

At high frequencies $\widehat{F}(\Omega)$ is approximately equal to $(-i\Omega)^{1/2}$, which corresponds to the half-derivative operator $\left(\frac{\partial}{\partial\sigma}\right)^{1/2}$, equal to the $\left(t_n\frac{\partial}{\partial t_n}\right)^{1/2}$ term of the asymptotic OC operator (9). The difference between the exact filter $\widehat{F}$ and its approximation by the half-order derivative operator is shown in Figure 3. This difference is an actual measure of the validity of asymptotic OC operators.

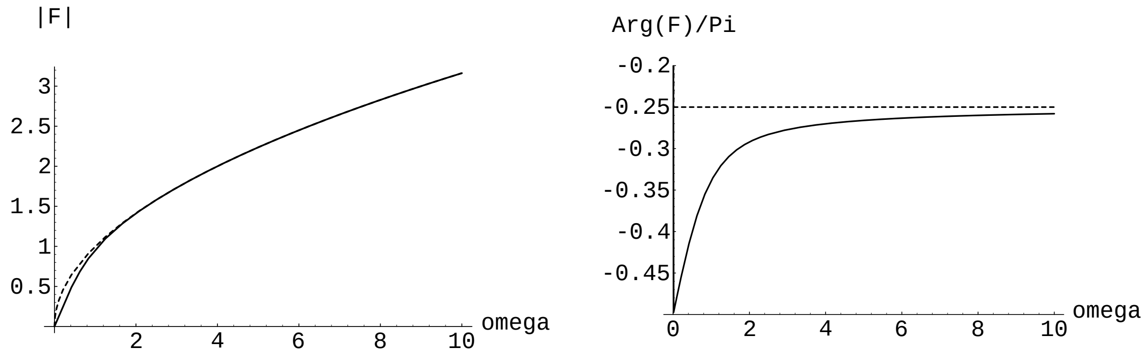


Figure 3: Amplitude (left) and phase (right) of the time filter in the log-stretch domain. The solid line is for the exact filter; the dashed line, for its approximation by the half-order derivative filter. sergey1-offflt [CR]

Inverting operator (45), we can obtain the DMO operator in the $\{\Omega, y\}$ domain.

## CONCLUSIONS

I have constructed integral offset continuation operators by posing and solving an initial value problem for the offset continuation equation (1). For the special cases of continuation to zero offset (DMO) and continuation from zero offset (inverse DMO) the OC operators are related to the known forms of DMO operators: Hale's Fourier DMO, Born DMO, and Liner's "exact log DMO." The discovery of these relations sheds additional light on the problem of amplitude preservation in DMO.

The wave-type process, described by equation (1), contains two different branches, associated with continuation to either larger or smaller offsets. In order to separate the desired (one-way) direction of continuation, one needs to use the first-order derivative of the recorded wavefield with respect to the offset. This requirement is eliminated in the case of inverse DMO, where the offset derivative vanishes to zero according to the reciprocity principle. I propose inverting the amplitude-preserving inverse DMO as a way to create the true-amplitude DMO operator.

In Part Three of this paper, I plan to describe a method of eliminating the first-derivative requirement in the general case of offset continuation. This method will allow me to proceed from the theory of amplitude preserving offset continuation to synthetic tests and real data applications.

## ACKNOWLEDGMENTS

I acknowledge the support of Alexey Stovas, who introduced me to the world of DMO and proposed the idea of Appendix C. Shuki Ronen and Richard Bale drew my attention to the importance of the log-stretch domain in DMO and related problems. I thank David Lumley for his thorough proofreading and useful suggestions.

## REFERENCES

Bagaini, C., and Spagnolini, U., 1993, Common shot velocity analysis by shot continuation operator: 63th Ann. Internat. Mtg., Soc. Expl. Geophys., Expanded Abstracts, 673–676.

Bagaini, C., Spagnolini, U., and Pazienza, V., 1994, Velocity analysis and missing offset restoration by prestack continuation operators: 64th Ann. Internat. Mtg., Soc. Expl. Geophys., Expanded Abstracts, 1549–1552.

Bale, R., and Jakubowicz, H., 1987, Post-stack prestack migration: 57th Annual Internat. Mtg., Soc. Expl. Geophys., Expanded Abstracts, Session:S14.1.

Berg, L. A., 1985, Prestack partial migration: Presented at the EAEG Meeting.

Beylkin, G., 1985, Imaging of discontinuities in the inverse scattering problem by inversion of a causal generalized Radon transform: Journal of Mathematical Physics, **26**, 99–108.

Biondi, B., and Chemingui, N., 1994a, Transformation of 3-D prestack data by azimuth moveout (AMO): 64th Ann. Internat. Mtg., Soc. Expl. Geophys., Expanded Abstracts, 1541–1544.

Biondi, B., and Chemingui, N., 1994b, Transformation of 3-D prestack data by Azimuth Moveout: SEP–**80**, 125–143.

Black, J. L., Schleicher, K. L., and Zhang, L., 1993, True-amplitude imaging and dip moveout: Geophysics, **58**, no. 1, 47–66.

Bleistein, N., 1990, Born DMO revisited: 60th Annual Internat. Mtg., Soc. Expl. Geophys., Expanded Abstracts, 1366–1369.

Bolondi, G., Loinger, E., and Rocca, F., 1982, Offset continuation of seismic sections: Geophys. Prosp., **30**, no. 6, 813–828.

Chemingui, N., and Biondi, B., 1995, Amplitude preserving AMO from true amplitude DMO and inverse DMO: SEP–**84**, 153–168.

Courant, R., 1962, Methods of mathematical physics: Interscience Publishers, New York.

Deregowski, S. M., and Rocca, F., 1981, Geometrical optics and wave theory of constant offset sections in layered media: Geophys. Prosp., **29**, no. 3, 374–406.

Fomel, S., and Biondi, B., 1995, The time and space formulation of azimuth moveout: SEP–**82**, 25–37.

Fomel, S. B., 1994, Kinematically equivalent differential operator for offset continuation of seismic sections: Russian Geology and Geophysics, **35**, no. 9, 122–134.

Fomel, S., 1995, Amplitude preserving offset continuation in theory. Part 1: The offset continuation equation: SEP–**84**, 179–196.

Goldin, S. V., 1988, Transformation and recovery of discontinuities in problems of tomographic type: Institute of Geology and Geophysics, Novosibirsk (in Russian).

Goldin, S., 1990, A geometric approach to seismic processing: the method of discontinuities: SEP–**67**, 171–210.

Gradshtein, I. S., and Ryzhik, I. M., 1994, Table of integrals, series, and products: Boston: Academic Press.

Hale, I. D., 1983, Dip moveout by Fourier transform: Ph.D. thesis, Stanford University.

Hale, D., 1984, Dip-moveout by Fourier transform: Geophysics, **49**, no. 6, 741–757.

Hale, D., 1991a, A nonaliased integral method for dip moveout: Geophysics, **56**, no. 6, 795–805.

Hale, D., 1991b, Course notes: Dip moveout processing: Soc. Expl. Geophys., Tulsa.

Liner, C. L., and Cohen, J. K., 1988, An amplitude-preserving inverse of Hale's DMO: 58th Annual Internat. Mtg., Soc. Expl. Geophys., Expanded Abstracts, 1117–1120.

Liner, C., 1990, General theory and comparative anatomy of dip moveout: Geophysics, **55**, no. 5, 595–607.

Liner, C. L., 1991, Born theory of wave-equation dip moveout: Geophysics, **56**, no. 2, 182–189.

Notfors, C. D., and Godfrey, R. J., 1987, Dip moveout in the frequency-wavenumber domain (short note): Geophysics, **52**, no. 12, 1718–1721.

Ronen, S., Sorin, V., and Bale, R., 1991, Spatial dealiasing of 3-D seismic reflection data: Geophysical Journal International, pages 503–511.

Ronen, J., 1987, Wave equation trace interpolation: Geophysics, **52**, no. 7, 973–984.

Ronen, S., 1994, Handling irregular geometry: Equalized DMO and beyond: 64th Ann. Internat. Mtg., Soc. Expl. Geophys., Expanded Abstracts, 1545–1548.

Schwab, M., 1993, Shot gather continuation: SEP–**77**, 117–130.

Stovas, A. M., and Fomel, S. B., 1993, Kinematically equivalent DMO operators: Presented at the SEG-Moscow.

Watson, G. N., 1952, A treatise on the theory of Bessel functions: Cambridge University Press, 2nd edition.

## APPENDIX A

## SOLVING THE CAUCHY PROBLEM

To obtain an explicit solution of the Cauchy problem (1)-(3), it is convenient to apply the following simple transform of the function $P$:

$$P(t_n,h,y) = Q(t_n,h,y)\, t_n\, H(t_n)\;. \tag{A-1}$$

Here the Heavyside function $H$ is included to take into account the causality of the reflection seismic gathers (note that the time $t_n = 0$ corresponds to the direct wave arrival). We can evenly extrapolate the function $Q$ to negative times, writing the reverse of (A-1) as follows:

$$Q(t_n,h,y) = Q(-t_n,h,y) = P(|t_n|,h,y)/|t_n|\;. \tag{A-2}$$

With the change of function (A-1), equation (1) transforms to

$$h\,\frac{\partial^2 Q}{\partial y^2} = h\,\frac{\partial^2 Q}{\partial h^2} + t_n\,\frac{\partial^2 Q}{\partial t_n\,\partial h} + \frac{\partial Q}{\partial h} = \frac{\partial}{\partial h}\left(h\,\frac{\partial Q}{\partial h} + t_n\,\frac{\partial Q}{\partial t_n}\right)\;. \tag{A-3}$$

Applying the change of variables

$$\rho = \frac{t_n^2}{2} \; , \; \nu = \frac{h^2}{2\, t_n^2} \tag{A-4}$$

and Fourier transform in the midpoint coordinate $y$

$$\widetilde{Q}(\rho,\nu) = \int Q(\rho,\nu,y)\, \exp(-iky)\, dy \; , \tag{A-5}$$

I further transform equation (A-3) to the canonical form of a hyperbolic-type partial differential equation with two variables:

$$\frac{\partial^2 \widetilde{Q}}{\partial\rho\, \partial\nu} + k^2\, \widetilde{Q} = 0 \; . \tag{A-6}$$

The initial value conditions (2) and (3) in the $\{\rho,\nu\}$ space are defined on a hyperbola of the form $\rho\,\nu = \left(\frac{h_1}{2}\right)^2 =$ constant. Now the solution of the Cauchy problem follows directly from Riemann's method (Courant, 1962). According to this method, the domain of dependence of each point $\{\rho,\nu\}$ is a part of the hyperbola between the points $\{\rho, \frac{h_1^2}{4\,\nu}\}$ and $\{\frac{h_1^2}{4\,\rho}, \nu\}$ (Figure A-1). If we let $\Sigma$ denote this curve, the solution takes an explicit integral form:

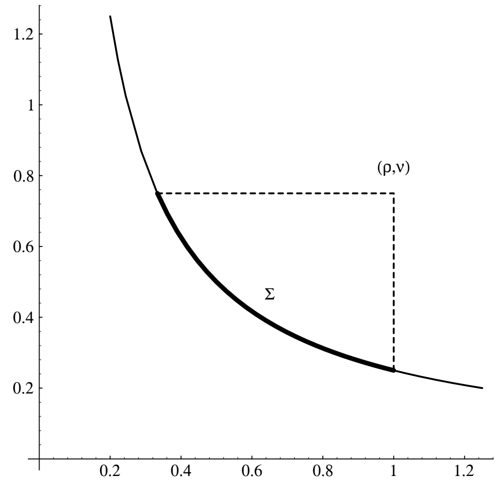


Figure A-1: Domain of dependence of a point in the transformed coordinate system. sergey1-offrim [CR]

$$\widetilde{Q}(\rho,\nu) = \frac{1}{2}\, \widetilde{Q}(\rho, \frac{h_1^2}{4\,\nu}) + \frac{1}{2}\, \widetilde{Q}(\frac{h_1^2}{4\,\rho}, \nu) + \tag{A-7}$$

$$+\frac{1}{2} \int_\Sigma \left( R(\rho_1,\nu_1;\rho,\nu)\, \frac{\partial \widetilde{Q}(\rho_1,\nu_1)}{\partial \rho_1} - \widetilde{Q}(\rho_1,\nu_1)\, \frac{\partial R(\rho_1,\nu_1;\rho,\nu)}{\partial \rho_1} \right) d\rho_1 - \tag{A-8}$$

$$-\frac{1}{2} \int_\Sigma \left( R(\rho_1,\nu_1;\rho,\nu)\, \frac{\partial \widetilde{Q}(\rho_1,\nu_1)}{\partial \nu_1} - \widetilde{Q}(\rho_1,\nu_1)\, \frac{\partial R(\rho_1,\nu_1;\rho,\nu)}{\partial \nu_1} \right) d\nu_1 \; . \tag{A-9}$$

Here $R$ is the Riemann's function of equation (A-6), which has the known explicit analytical expression

$$R(\rho_1,\nu_1;\rho,\nu) = J_0\left(2k\sqrt{(\rho_1-\rho)\;(\nu_1-\nu)}\right)\;, \tag{A-10}$$

where $J_0$ is Bessel's function of zero order. Integrating by parts and taking into account the connection of the variables on the curve $\Sigma$, we can simplify formula (A-9) to the form

$$\widetilde{Q}(\rho,\nu) = \widetilde{Q}_0(\rho,\nu) + \widetilde{Q}_1(\rho,\nu)\;, \tag{A-11}$$

where

$$\widetilde{Q}_0(\rho,\nu) = \frac{\partial}{\partial\rho}\int_\Sigma R(\rho_1,\nu_1;\rho,\nu)\,\widetilde{Q}(\rho_1,\nu_1)\,d\rho_1\;, \tag{A-12}$$

$$\widetilde{Q}_1(\rho,\nu) = -\int_\Sigma R(\rho_1,\nu_1;\rho,\nu)\,\frac{\partial\widetilde{Q}(\rho_1,\nu_1)}{\partial\nu_1}\,d\nu_1\;. \tag{A-13}$$

Applying the explicit expression for the Riemann's function $R$ (A-10) and performing the inverse transform of both the function and the variables allows us to rewrite equations (A-11), (A-12), and (A-13) in the original coordinate system. This yields the integral offset continuation operators in the $\{t_n,h,k\}$ domain

$$\widetilde{P}(t_n,h,k) = H(t_n)\,\left(\widetilde{P}_0(t_n,h,k) + t_n\,\widetilde{P}_1(t_n,h,k)\right)\;, \tag{A-14}$$

where

$$\widetilde{P}_0 = \frac{\partial}{\partial t_n}\int_{(h_1/h)\,t_n}^{t_n}\widetilde{P}_1^{(0)}\left(|t_1|\,,k\right)\;J_0\left(k\sqrt{\left(\frac{h^2}{t_n^2}-\frac{h_1^2}{t_1^2}\right)\;(t_n^2-t_1^2)}\right)\,dt_1\;, \tag{A-15}$$

$$\widetilde{P}_1 = \int_{(h_1/h)\,t_n}^{t_n} h_1\,\widetilde{P}_1^{(1)}\left(|t_1|\,,k\right)\;J_0\left(k\sqrt{\left(\frac{h^2}{t_n^2}-\frac{h_1^2}{t_1^2}\right)\;(t_n^2-t_1^2)}\right)\,\frac{dt_1}{t_1^2}\;, \tag{A-16}$$

$$\widetilde{P}_1^{(j)}(t_1,k) = \int P_1^{(j)}(t_1,y_1)\exp(-iky_1)\,dy_1\;(j=0,1)\;, \tag{A-17}$$

$$\widetilde{P}(t_n,h,k) = \int P(t_n,h,y)\exp(-iky)\,dy\;(j=0,1)\;. \tag{A-18}$$

The inverse Fourier transforms of formulas (A-15) and (A-16) are reduced to analytically evaluated integrals (Gradshtein and Ryzhik, 1994) to produce explicit integral operators in the time-and-space domain

$$P(t_n,h,y) = \mathrm{sign}(h-h_1)\,\frac{H(t_n)}{\pi}\,\left(P_0(t_n,h,y) + t_n\,P_1(t_n,h,y)\right)\;, \tag{A-19}$$

where

$$P_0(t_n,h,y) = \frac{\partial}{\partial t_n} \iint_\Sigma \frac{P_1^{(0)}\left(\left|t_1\right|,y_1\right)\,dt_1\,dy_1}{\sqrt{\left(\frac{h^2}{t_n^2}-\frac{h_1^2}{t_1^2}\right)\,\left(t_n^2-t_1^2\right)-\left(y-y_1\right)^2}}\;, \tag{A-20}$$

$$P_1(t_n,h,y) = \iint_\Sigma \frac{\left(h_1/t_1^2\right)\,P_1^{(1)}\left(\left|t_1\right|,y_1\right)\,dt_1\,dy_1}{\sqrt{\left(\frac{h^2}{t_n^2}-\frac{h_1^2}{t_1^2}\right)\,\left(t_n^2-t_1^2\right)-\left(y-y_1\right)^2}}\;. \tag{A-21}$$

The range of integration $\Sigma$ in (A-20) and (A-21) is defined by inequality

$$\Theta(t_1,h_1,y_1;t_n,h,y) > 0\;, \tag{A-22}$$

where $\Theta$ is in turn defined by formula (7). Formulas (A-19), (A-20), and (A-21) coincide with (4), (5), and (6) in the main text.

## APPENDIX B

## THE KINEMATICS OF OFFSET CONTINUATION

In this Appendix, I apply an alternative method to derive formula (10), which describes the summation path of the integral OC operator. The method is based on the following considerations.

The summation path of an integral (stacking) operator coincides with the phase function of the impulse response of the inverse operator. Impulse response is by definition the operator reaction to an impulse in the input data. For the case of offset continuation, the input is a reflection common-offset gather. From the physical point of view, an impulse in this type of data corresponds to the special focusing reflector (elliptical isochrone) at the depth. Therefore, reflection from this reflector at a different constant-offset corresponds to the impulse response of the OC operator. In other words, we can view offset continuation as the result of cascading prestack common-offset migration, which produces the elliptic surface, and common-offset modeling (inverse migration) for different offsets. This approach resemble that of Deregowski and Rocca (1981). It was applied recently to a more general case of azimuth moveout (AMO) by Fomel and Biondi (1995). The geometric approach implies that in order to find the summation pass of the OC operator, one should solve the kinematic problem of reflection from an elliptic reflector, whose focuses are in the shot and receiver locations of the output seismic gather.

In order to solve this problem , let us consider an elliptic surface of the general form

$$h(x) = \sqrt{d^2-\beta\left(x-x'\right)^2}\;, \tag{B-1}$$

where $\beta$ is less than 1. In a constant velocity medium, the reflection ray path for a given source-receiver pair on the surface is controlled by the position of the reflection point $x$. Fermat's principle provides a required constraint for finding this position. According to Fermat's principle, the reflection ray path corresponds to an extremum value of the travel-time. Therefore, in the neighborhood of this path,

$$\frac{\partial \tau(s,r,x)}{\partial x} = 0 \;, \tag{B-2}$$

where $s$ and $r$ stand for the source and receiver locations on the surface, and $\tau$ is the reflection traveltime

$$\tau(s,r,x) = \frac{\sqrt{h^2(x)+(s-x)^2}}{v} + \frac{\sqrt{h^2(x)+(r-x)^2}}{v} \;. \tag{B-3}$$

Substituting (B-3) and (B-1) into (B-2) leads to a quadratic algebraic equation on the reflection point parameter $x$. This equation has the explicit solution

$$x(s,r) = x' + \frac{\xi^2 + H^2 - h^2 + \mathrm{sign}(h^2 - H^2)\sqrt{\left(\xi^2 - H^2 - h^2\right)^2 - 4\,H^2\,h^2}}{2\,\xi\,(1-\beta)} \;, \tag{B-4}$$

where $h = (r-s)/2$, $\xi = y - x'$, $y = (s+r)/2$, and $H^2 = d^2\left(\frac{1}{\beta} - 1\right)$. Replacing $x$ in formula (B-3) with its expression (B-4) solves the kinematic part of the problem, producing the explicit traveltime expression

$$\tau(s,r) = \left\{ \begin{array}{ll} \frac{1}{v}\sqrt{\frac{4\,h^2 - \beta\,(f+g)^2}{1-\beta}} & \text{for} \quad h^2 > H^2 \\ \\ \frac{1}{v}\sqrt{\frac{4\,h^2 + \beta\,(F+G)^2}{1-\beta}} & \text{for} \quad h^2 < H^2 \end{array} \right. \;, \tag{B-5}$$

where

$$f = \sqrt{(r-x')^2 - H^2}\;,\; g = \sqrt{(s-x')^2 - H^2}\;,$$
$$F = \sqrt{H^2 - (r-x')^2}\;,\; G = \sqrt{H^2 - (s-x')^2}\;.$$

Two branches of formula (B-5) correspond to the difference in the geometry of the reflected rays in two different situations. When a source-and-receiver pair is inside the focuses of the elliptic reflector, the midpoint $y$ and the reflection point $x$ are on the same side of the ellipse with respect to its small semi-axis. They are on different sides in the opposite case (Figure B-1).

If we apply the NMO correction, formula (B-5) is transformed to

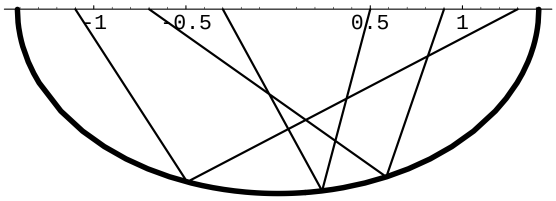


Figure B-1: Reflections from an ellipse. The three pairs of reflected rays correspond to a common midpoint (at 0.1) and different offsets. The focuses of the ellipse are at 1 and -1. sergey1-offell [CR]

$$\tau_n(s,r) = \left\{ \begin{array}{ll} \frac{1}{v}\sqrt{\frac{\beta}{1-\beta}}\,\sqrt{4\,h^2-(f+g)^2} & \mbox{for} \quad h^2 > H^2 \\ \\ \frac{1}{v}\sqrt{\frac{\beta}{1-\beta}}\,\sqrt{4\,h^2+(F+G)^2} & \mbox{for} \quad h^2 < H^2 \end{array} \right. . \tag{B-6}$$

Then, recalling the relationships between the parameters of the focusing ellipse $r$, $x'$ and $\beta$ and the parameters of the output seismic gather (Deregowski and Rocca, 1981)

$$r = \frac{v\,t_n}{2}\;,\; x' = y\;,\; \beta = \frac{t_n^2}{t_n^2+\frac{4\,h^2}{v^2}}\;,\; H = h\;, \tag{B-7}$$

and substituting expressions (B-7) into formula (B-6) yields the expression

$$t_1(s_1,r_1;s,r,t_n) = \left\{ \begin{array}{ll} \frac{t_n}{2\,h}\,\sqrt{4\,h_1^2-(f+g)^2} & \mbox{for} \quad h_1^2 > h^2 \\ \\ \frac{t_2}{2\,h}\,\sqrt{4\,h_1^2+(F+G)^2} & \mbox{for} \quad h_1^2 < h^2 \end{array} \right. , \tag{B-8}$$

where

$$f = \sqrt{(r_1-r)\,(r_1-s)}\;,\; g = \sqrt{(s_1-r)\,(s_1-s)}\;,$$
$$F = \sqrt{(r-r_1)\,(r_1-s)}\;,\; G = \sqrt{(s_1-r)\,(s-s_1)}\;.$$

It is easy to verify algebraically the mathematical equivalence of equation (B-8) and equation (10) in the main text. The kinematic approach described in this appendix applies equally well to different acquisition configurations of the input and output data. The source-receiver parameterization used in (B-8) is the actual definition for the summation path of the integral shot continuation operator (Schwab, 1993; Bagaini and Spagnolini, 1993). A family of these summation curves is shown in Figure B-2.

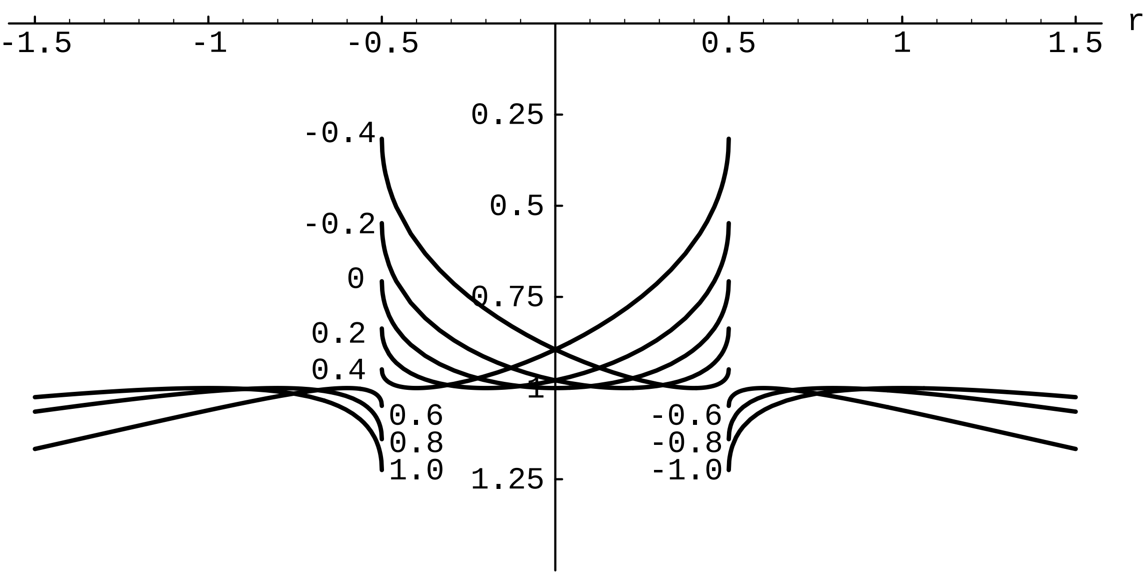


Figure B-2: Summation paths of the integral shot continuation. The output source is at -0.5 km. The output receiver is at 0.5 km. The indexes of the curves correspond to the input source location. sergey1-offshc [CR]

## APPENDIX C

## THE IMPULSE RESPONSE OF HALE'S DMO OPERATOR

The purpose of this appendix is to explain the apparent difference between Hale's DMO operator (Hale, 1984) and operator (17), which is the first term in the offset continuation to zero offset. The difference between the two operators is simply the real part of Hale's DMO. Therefore, I will analyze the real and the imaginary part separately and discuss the contributions of each. In order to do this, I derive the impulse response of Hale's DMO in the time-and-space domain, following the results of Stovas and Fomel (1993). The high-frequency asymptotics of the impulse response has been investigated previously in a number of publications (Berg, 1985; Liner, 1990; Hale, 1991a). Here we will obtain an exact formula, containing both high-frequency and low-frequency components.

Starting from Hale's DMO operator (Hale, 1984)

$$\widetilde{\widetilde{P}}_0(\omega_0, k) = \int_{-\infty}^{\infty} A^{-1}\, \widetilde{P}_1^{(0)}\left(|t_1|\,, k\right)\, \exp\left(i\omega_0\, t_1\, A\right)\, dt_1\ , \tag{C-1}$$

let us define its impulse response as a function $G(t_0, t_1, y)$ such that

$$P_0(t_0, y_0) = \iint P_1^{(0)}(t_1, y_0 - \xi)\, G(t_0, t_1, \xi)\, dt_1\, d\xi\ . \tag{C-2}$$

According to this definition, the impulse response of operator (C-1) can be expressed as

$$G = \frac{1}{(2\,\pi)^2} \int\!\!\int A^{-1}\,\widetilde{P}_1^{(0)}\left(|t_1|\,,k\right)\,\exp\left(i\omega_0\,(t_1\,A - t_0)\right)\,\exp(iky)\,d\omega_0\,dk\;. \tag{C-3}$$

Recalling the definition of Hale's factor $A$ (19) and changing the order of integration in the double integral, we can then rewrite expression (C-3) to the form

$$G = \frac{1}{(2\,\pi)^2} \int_{-\infty}^{\infty} \exp(-i\omega_0\,t_0)\,a \int \frac{\exp\left(i\hat{h}_1\sqrt{k^2+a^2}\right)}{\sqrt{k^2+a^2}}\,\exp(iky)\,dk\,d\omega_0\;, \tag{C-4}$$

where $\hat{h}_1 = h_1\,\mathrm{sign}(\omega_0)$, and $a = \frac{\omega_0\,t_1}{\hat{h}_1}$.

The inner integral in (C-4) is a known definite integral, evaluated explicitly in terms of cylinder functions (Gradshtein and Ryzhik, 1994). The idea of applying cylinder functions to the evaluation of the DMO impulse response was used previously by Berg (1985) and Hale (1991). After evaluation of the inner integral, expression (C-4) transforms to

$$G = \frac{i}{2\,\pi} \int_{-\infty}^{\infty} \exp(-i\omega_0\,t_0)\,\frac{a}{2}\,Z\left(a\,\sqrt{h^2-y^2}\right)\,d\omega_0\;, \tag{C-5}$$

where

$$Z(x) = \left\{ \begin{array}{ll} H_0^{(1)}(x) = J_0(x) + iY_0(x) & \text{for} \quad \omega_0 > 0 \\ \\ -H_0^{(2)}(x) = -J_0(x) + iY_0(x) & \text{for} \quad \omega_0 < 0 \end{array} \right. \;, \tag{C-6}$$

$H_0^{(1)}$ and $H_0^{(2)}$ are Hankel functions of zero order, and $J_0$ and $Y_0$ are, respectively, Bessel function and Weber function of zero order. Separating the real and the imaginary parts of the integrand transforms expression (C-5) to the form

$$G = i\frac{t_1}{2\,\pi\,h_1}\,\left[\int_0^{\infty} \exp(-i\omega_0\,t_0)\,H_0^{(1)}\left(\omega_0\,\hat{\theta}\right)\,\omega_0\,d\omega_0 - \right.$$

$$\left. - \int_0^{\infty} \exp(i\omega_0\,t_0)\,H_0^{(2)}\left(\omega_0\,\hat{\theta}\right)\,\omega_0\,d\omega_0\right] =$$

$$= -\frac{t_1}{2\,\pi\,h_1}\,\frac{\partial}{\partial t_0}\,\left[\int_0^{\infty} cos(\omega_0\,t_0)\,J_0\left(\omega_0\,\hat{\theta}\right)\,d\omega_0 + \right.$$

$$+ \int_0^{\infty} \sin(\omega_0\, t_0)\, Y_0\left(\omega_0\, \hat{\theta}\right)\, d\omega_0 \Bigg] \;, \tag{C-7}$$

where

$$\hat{\theta} = t_1 \sqrt{1 - \frac{y^2}{h_1^2}}\;. \tag{C-8}$$

Note that the Bessel function in the first term of formula (C-7) follows from the real part of the Hankel function, which is in turn connected with the imaginary part of Hale's operator (C-1). For the same reason, the second term in formula (C-7) is the contribution from the real part of operator (C-1). Both definite integrals in (C-7) have known analytical expressions listed in integral tables (Gradshtein and Ryzhik, 1994). With the help of these expressions, the first term is expressed as

$$G^1(t_0, t_1, y) = -\frac{t_1}{\pi\, h_1}\, \frac{\partial}{\partial t_0} \left(\frac{H(\hat{\theta}^2 - t_0^2)}{\sqrt{\hat{\theta}^2 - t_0^2}}\right) \;, \tag{C-9}$$

while the second term transforms to

$$G^2(t_0, t_1, y) = -\frac{t_1}{\pi^2\, h_1}\, \frac{\partial}{\partial t_0} \left\{ \begin{array}{ll} \dfrac{\arcsin(t_0/\hat{\theta}) - \pi/2}{\sqrt{\hat{\theta}^2 - t_0^2}} & \text{for} \quad t_0 < \hat{\theta} \\ \\ \dfrac{\ln\left(t_0/\hat{\theta} - \sqrt{\left(t_0/\hat{\theta}\right)^2 - 1}\right)}{\sqrt{t_0^2 - \hat{\theta}^2}} & \text{for} \quad t_0 > \hat{\theta} \end{array} \right. \;. \tag{C-10}$$

The first term ($G^1$) is discontinuous on the line $t_0 = \hat{\theta}$, which is the known form of the DMO impulse response (Deregowski and Rocca, 1981), while the second term ($G^2$) is continuous and smooth everywhere. In order to prove this fact, one can easily verify that both the left-sided and right-sided limits of expression (C-10) for $t_0$ approaching $\hat{\theta}$ are

$$\lim_{t_0 \to \hat{\theta} - 0} G^2 = \lim_{t_0 \to \hat{\theta} + 0} G^2 = -\frac{t_1}{3\,\pi^2\, h_1\, t_0^2} \;, \tag{C-11}$$

and the limits of its derivative are

$$\lim_{t_0 \to \hat{\theta} - 0} \frac{\partial G^2}{\partial t_0} = \lim_{t_0 \to \hat{\theta} + 0} \frac{\partial G^2}{\partial t_0} = \frac{4\, t_1}{15\,\pi^2\, h_1\, t_0^3}\;. \tag{C-12}$$

The second (smooth) term of the impulse response, which comes from the real part of Hale's DMO, obviously does not contribute to the imaging properties of DMO.

Moreover, it continues non-causally (and with monotonical growth) to the negative times (Figure C-1), which contradicts the sense of DMO (and offset continuation) as an operator defined for positive times only. The energy of the second term is almost negligible, especially with respect to the high-frequency asymptotics. Therefore, in practice its presence doesn't affect the DMO behavior much. The conclusion that is made in this Appendix justifies the absence of this term in the DMO operator derived from the amplitude-preserving offset continuation (17).

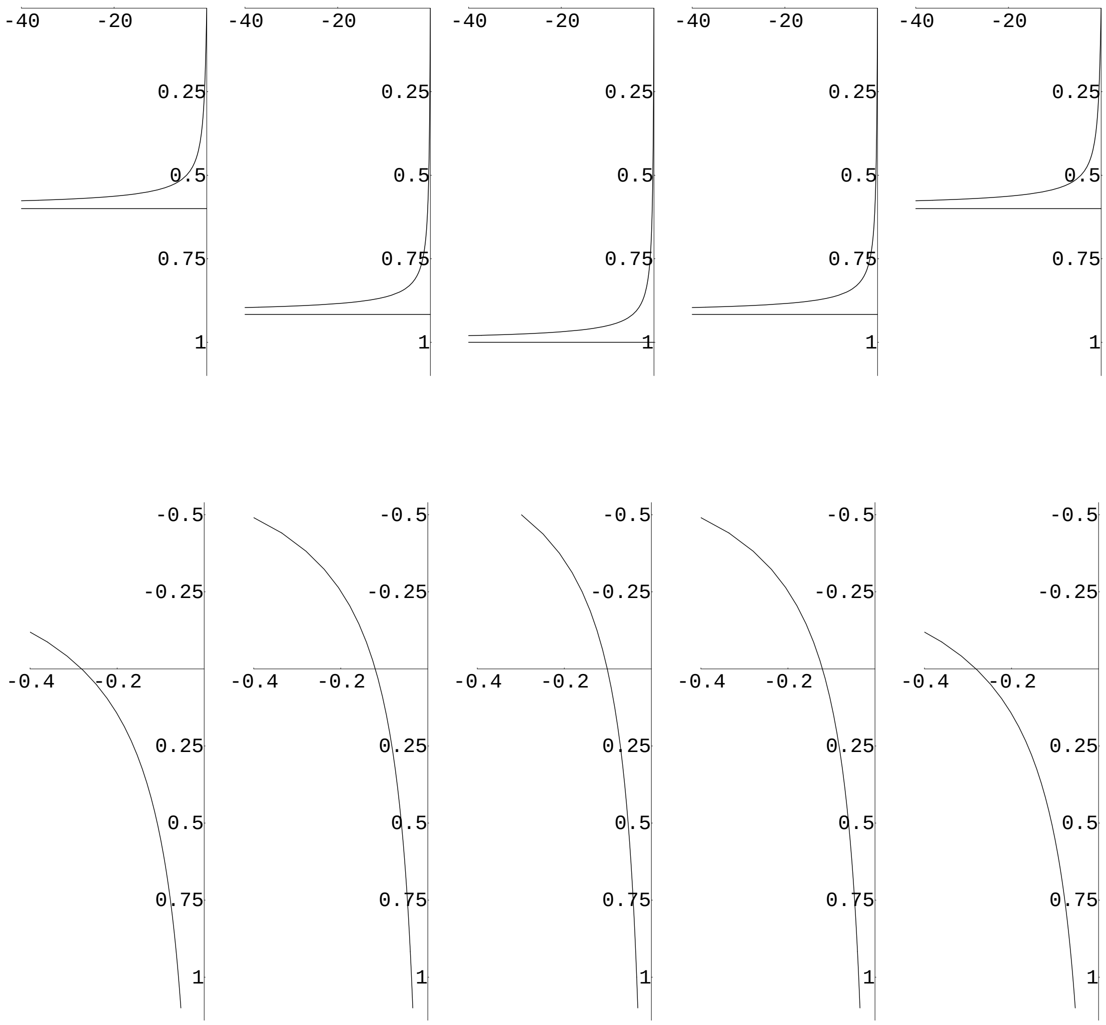


Figure C-1: Theoretical impulse response of Hale's DMO. Top: impulse response of the imaginary part; bottom: impulse response of the real part. Note the scale difference. sergey1-offimp [CR]